ACS APPLIED NANO MATERIALS

www.acsanm.org Article

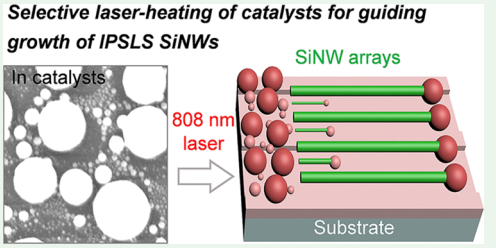
Growth Control of In-Plane Silicon Nanowires via Catalyst Size-Dependent Laser Heating for High-Performance Electronics

Yinzi Cheng, Zongguang Liu,* Ruijin Hu, Junzhuan Wang, Jun Xu, and Linwei Yu*

Cite This: ACS Appl. Nano Mater. 2024, 7, 16874−16882 Read Online

ACCESS | Metrics & More | Article Recommendations | Supporting Information

ABSTRACT: The in-plane growth of high-quality crystalline silicon nanowires (SiNWs) guided by laser-heated metal catalysts provides a solid one-dimensional channel material for the integration of high-performance Si-based electronics, while the growth control of these SiNWs remains an unexplored problem. In this study, we demonstrate that the laser-heated growth of IPSLS SiNWs can be modulated by the diameter of leading catalysts. The large catalysts with a diameter of ∼220 nm were directly heated under continuous laser illumination by a typical selected laser-droplet-heating mode, which resulted in the rapid growth of high-quality SiNWs with a large diameter of 166 ± 27 nm. Conversely, the small catalysts (diameter of <130 nm) can only be activated by the underlying silicon substrate heated under laser illumination, allowing the rapid growth of thin SiNWs of 74 ± 9 nm within 30 s. The different growth modes can be explained by a size-dependent heating theory of nanoscale catalysts with laser illumination. This study proposes a comprehensive understanding of the growth and diameter control of in-plane SiNWs under laser illumination, providing high-quality channel arrays for the construction of Si-based electronics.



KEYWORDS: *indium droplets, nanowire integration, IPSLS growth, diameter control, NIR laser, selective growth*

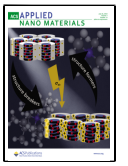
INTRODUCTION

Silicon nanowires (SiNWs) are one of the most important quasi-one-dimensional semiconductor channel materials for building a new generation of high-performance electronic logic,[1,2] thin-film transistors,[3−5] and chemical or biosensors,[6−10] due to its unique slim structure, large surface-to-volume ratio, and excellent transport characteristics.[11] Currently, the reliable fabrication and integration of crystalline SiNW channels are usually accomplished by state-of-the-art top-down etching techniques, including expensive electron beam lithography (EBL),[12] deep ultraviolet,[13,14] extreme ultraviolet lithography,[15] and self-aligned double patterning.[16,17] In addition, bottom-up catalytic growth of SiNWs guided by metal droplets (such as Ni, Au, and Sn) is a more cost-effective and simpler approach than that by complex top-down etching methods, for example, the well-known solid−liquid−solid (SLS)[18,19] and vapor−liquid−solid (VLS) growth methods.[20−22] Nevertheless, a significant obstacle to the growth of high-quality SiNWs is the necessity of temperatures usually >600 °C and the challenge of achieving precise nanowire positioning without the use of complex transfer processes.[23−25]

To address the self-localization challenge, we have developed an in-plane solid−liquid−solid (IPSLS) growth strategy in our previous study,[26−28] where the indium (In) catalyst droplets move along a predesigned guiding edge and absorb a hydrogenated amorphous Si (a-Si:H) layer to produce SiNW arrays, as illustrated in Figure 1a. The as-grown SiNWs have been widely applied in field effect transistors (FETs),[29−31] logic,[32] sensing,[33,34] and NEMS devices,.[35,36] Since the growth temperature in IPSLS mode is only required at the droplet level, we recently developed a self-selected laser-droplet-heating strategy to elevate temperature for the in-plane growth of high-quality SiNWs,[37] where the leading In droplets show much stronger absorption to infrared laser (808 nm) than those of the surrounding a-Si:H and glass or silicon wafer. Thanks to the direct heating of the leading droplets, the quality of the as-grown SiNWs has been proven to be equivalent to those produced with high-temperature (>600 °C) environmental heating. Importantly, these selective nanoscale In metal heaters allow the high heat to be localized in a submicrometer space, which opens an effective way to integrate high-quality NW channels directly upon polymer substrates for developing high-performance flexible electronics.

Considering the extremely small heat capacitance of the tiny catalyst droplets and droplet volume-dependent heating efficiency $\sim D_{In}^{3}$ (diameter of In droplet), the local temperature elevation of catalyst droplets under laser-heated mode could also be catalyst size-dependent. Different from the traditional substrate heating mode used in our previous works, where all of the droplets are heated and activated to guide the

Received: May 23, 2024
Revised: July 10, 2024
Accepted: July 11, 2024
Published: July 18, 2024



Downloaded from pubs.acs.org/aannf6/article-pdf/7/14/16874/4405546/an4c02962.pdf by NANJING UNIV user on 04 November 2026

© 2024 American Chemical Society

https://doi.org/10.1021/acsanm.4c02962
ACS Appl. Nano Mater. 2024, 7, 16874−16882

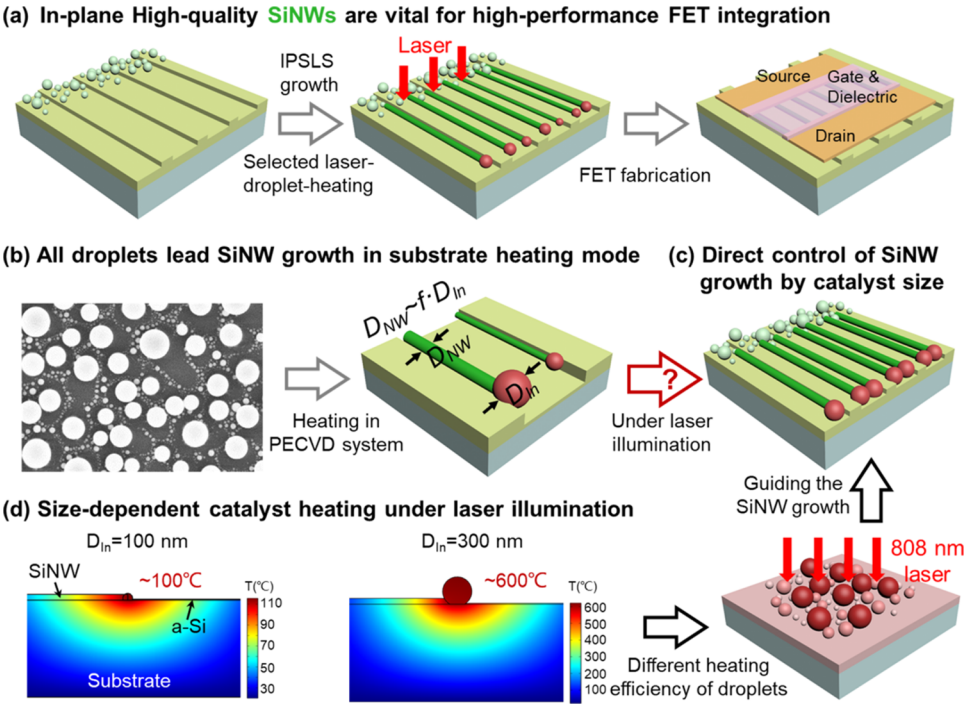


Figure 1. (a) High-quality IPSLS SiNW arrays grown by selected laser-droplet-heating mode are very important for high-performance FET integration. (b) All of the droplets are heated to guide the growth of SiNW in the traditional substrate heating mode in the PECVD system, with the $D_{NW} \sim fD_{In}$. (c) Growth control of SiNWs by catalyst size-dependent heating under laser illumination. (d) The results in COMSOL simulation indicated that the heating efficiency of the catalyst under laser illumination is size-dependent, where large droplets are easily heated to high temperature (~600 °C) for the guiding growth of SiNWs.

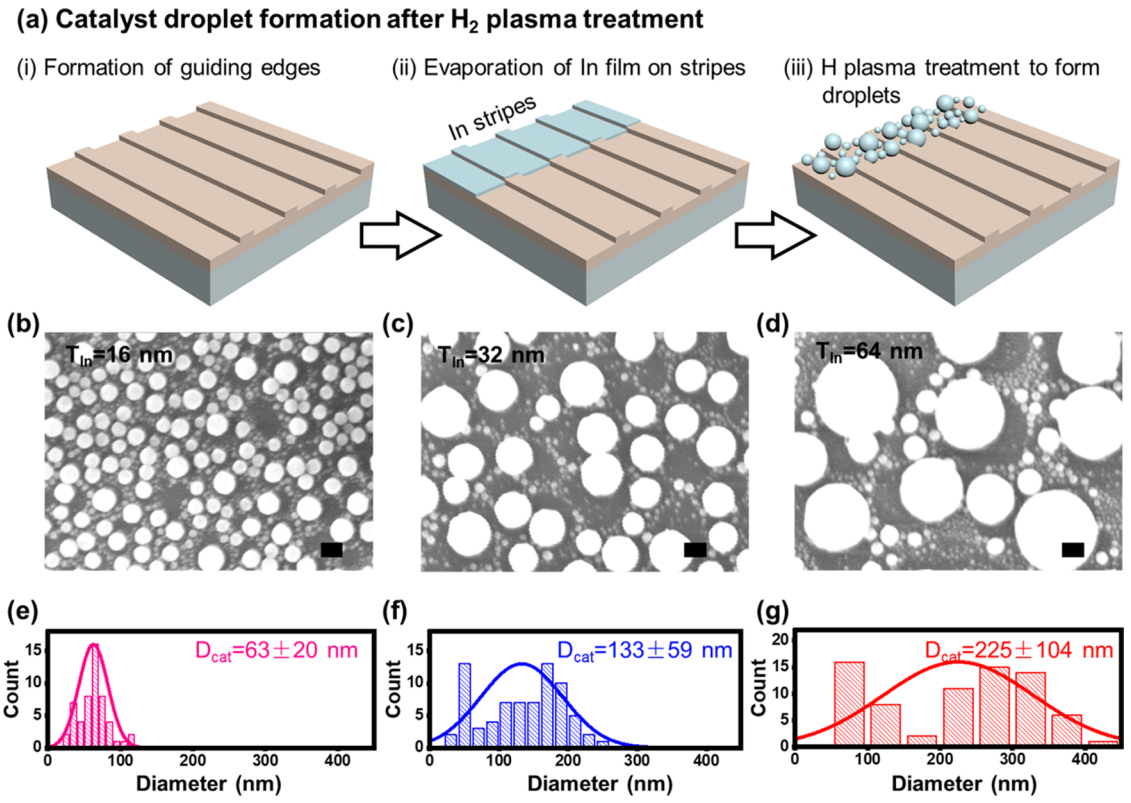


Figure 2. Catalyst droplet formation with different nominal thicknesses. (a) A schematic illustration of the formation of In droplets. The stripe region was first prepared by photolithography (i); then In catalyst stripe was formed by thermal evaporation and lift-off procedure (ii); the sample was loaded into PECVD and treated by H_2 plasma treatment to form spherical droplets (iii). (b–d) The morphology of as-received droplets with nominal catalyst thicknesses of 16, 32, and 64 nm. (e–g) The statistic of droplet distribution of different catalyst thicknesses. Scale bars in b–d stand for 100 nm.

https://doi.org/10.1021/acsanm.4c02962
ACS Appl. Nano Mater. 2024, 7, 16874−16882

Downloaded from pubs.acs.org/aanmf6/article-pdf/7/14/16874/4405546/an4c02962.pdf by NANJING UNIV user on 04 November 2026

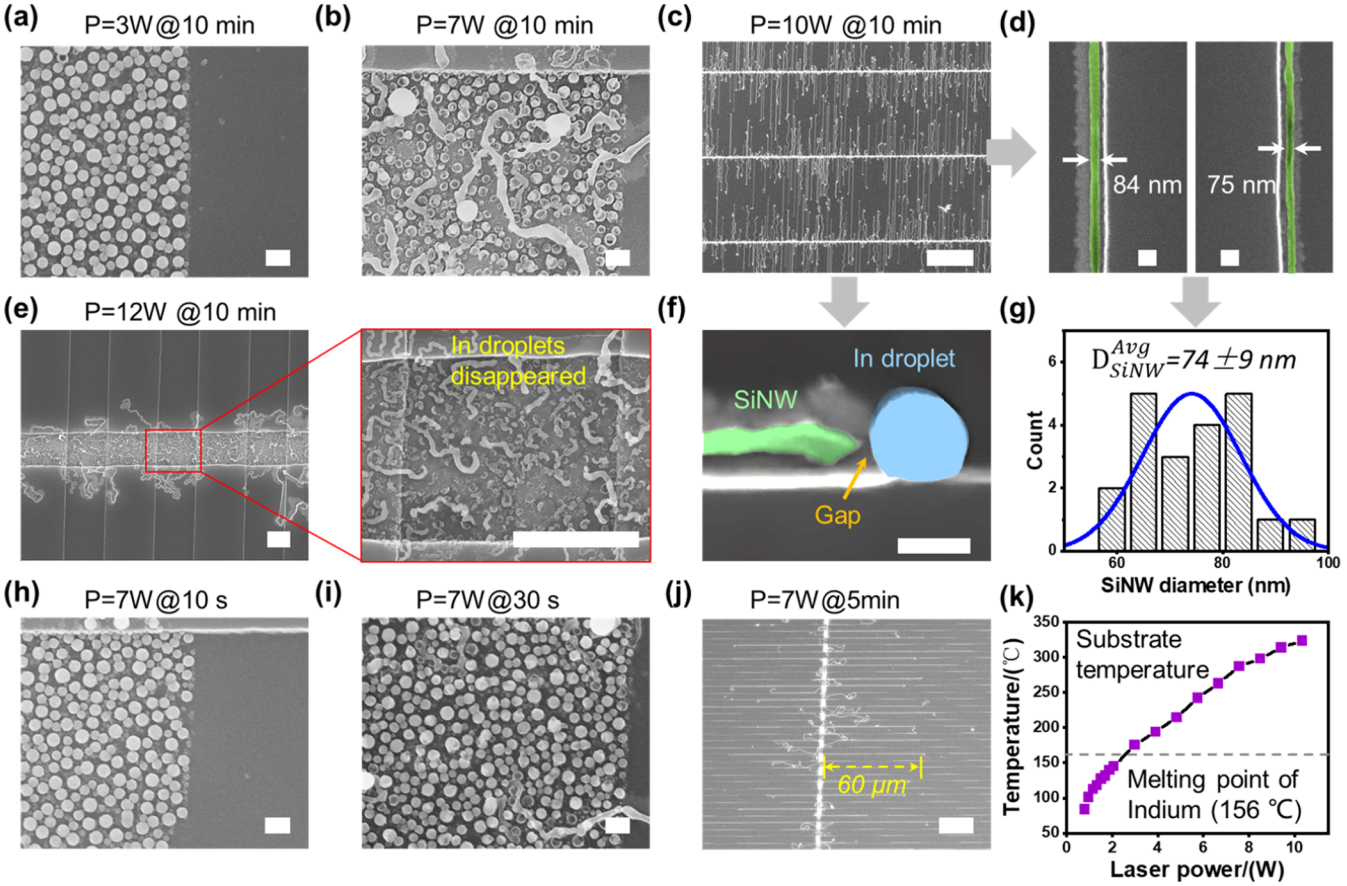


Figure 3. IPSLS growth of SiNWs led by catalysts with a diameter of ~60 nm under laser illumination. (a–c) and (e) The growth of SiNWs heated by 3, 7, 10, and 12 W of laser power for 10 min. (d) The middle segment of as-grown SiNWs after 10 W laser heating for 10 min, and the corresponding diameter statistics of SiNWs is shown in (g). (f) The image of growth end of SiNW, with a gap between the droplet and the SiNW. (h–j) The dynamic growth of SiNWs heated by 7 W of laser at growth times of 10 s, 30 s, and 5 min. (k) The curve of substrate temperature as a function of laser power. The temperature was recorded when it reached a steady-state value. Scale bars in (a), (b), (d), (f), (h), and (i) stand for 200 nm; in (c) for 100 μm; in (e) for 2 μm; and in (j) for 20 μm.

growth of SiNWs with diameters of $D_{NW} \sim f{\cdot}D_{In}$[25,38−40] (Figure 1b), the size-dependent heating in the laser heating mode may result in a different IPSLS SiNW growth (Figure 1c). However, this important aspect has never been verified experimentally. The heating capacity of In catalysts with different sizes under 808 nm laser illumination was first determined using COMSOL simulation toolkits, as shown in Figure 1d. The results indicated that the larger droplets (e.g., D_{In} = 300 nm) are indeed more readily heated to a high temperature (~600 °C) than smaller ones (D_{In} = 100 nm). This unique capacity thus inspires us that the large droplets can be quickly heated and guide the fast growth of SiNWs, while the surrounding smaller droplets remain at a relatively low temperature and suppress the growth of SiNWs (the right panel of Figure 1d).

In this work, we systematically investigated the heating effects and growth of SiNWs led by different catalyst sizes from the nominal thicknesses of 16, 32, and 64 nm. It was found that the larger catalyst droplets were directly heated by a laser, facilitating the guiding growth of high-quality SiNWs with large diameters via a laser-heated mode. Conversely, smaller droplets can only be heated by the substrate heat transferring mode, resulting in the leading growth of smaller SiNWs. This study provides a new and comprehensive understanding of the laser-droplet-SiNW growth process, which plays a vital role in the growth or diameter control of in-plane SiNWs and their integration into electronic devices.

RESULTS AND DISCUSSION

To better understand the absorption and heating capacity of catalyst droplets under NIR laser illumination, three samples with nominal catalyst thicknesses of 16, 32, and 64 nm were first prepared at the end of guiding edges by thermal evaporation (Figure 2a(i,ii)). Then, the samples were loaded into a plasma-enhanced chemical vapor deposition (PECVD) system and treated with H_2 plasma at 250 °C to remove the oxide layer of In and allow them to agglomerate into discrete droplets (Figure 2a(iii)). The SEM images in Figure 2b–d show that the sizes of obtained droplets increased with the increase of In thickness, with the statistical diameters of 63 ± 20, 133 ± 59, and 225 ± 104 nm (Figure 2e–g).

We first studied the IPSLS growth of SiNWs under laser illumination, led by the In catalyst droplets formed from an initial thickness of 16 nm. Before the SiNW growth, the amorphous silicon layer of ~20 nm thickness, commonly used for IPSLS growth of SiNWs,[33,41] was deposited as a precursor in the PECVD system, by controlling the deposition time of 4 min. Then, the 808 nm laser was applied to illuminate the samples to heat the catalysts for driving the growth of SiNWs along the guiding edge. During this course, the In droplets

https://doi.org/10.1021/acsanm.4c02962
ACS Appl. Nano Mater. 2024, 7, 16874−16882

Downloaded from pubs.acs.org/aanmf6/article-pdf/7/14/16874/4405546/an4c02962.pdf by NANJING UNIV user on 04 November 2026

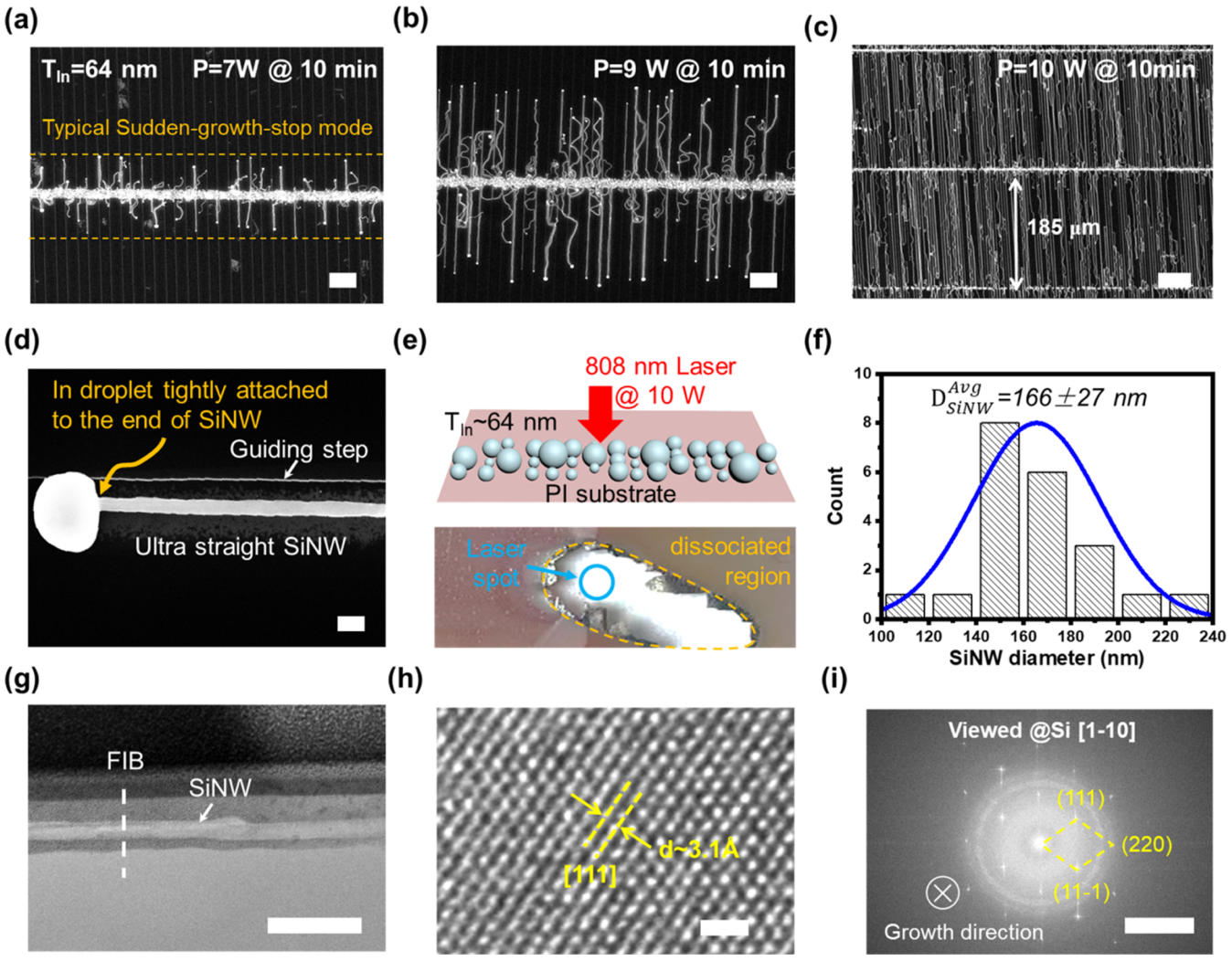


Figure 4. IPSLS growth of SiNW led by initial droplet diameter of ~220 nm from T_{In} of 64 nm under laser illumination. (a–c) The growth of SiNWs heated by different laser powers of 7, 9, and 10 W for 10 min, respectively. (d) The image of the growth end of SiNW, where the In droplet was tightly attached to the end of SiNW, indicating a fast cooling of droplet after the laser was off. (e) Dissociation of In-coated PI substrate after 10 W laser illumination. (f) The diameter statistics of SiNWs grown by 10 W laser heating. (g) TEM view of the selected area of SiNW for FIB etching. (h) HR-TEM image of the cross section of SiNW and the corresponding electron diffraction pattern is shown in (i). Scale bars in (a) and (b) stand for 10 μm; in (c) for 50 μm; in (d) for 500 nm; in (g) for 200 nm; in (h) for 1 nm; and in (i) for 51/nm.

became molten and started to absorb nearby a-Si to establish a supersaturation state in the droplet. Eventually, c-Si seeds will form preferentially at the bottom edges, joined by the liquid droplet and the substrate surface, and continue to grow larger and larger to tilt the droplet to move in the opposite direction. Since the amorphous thin film has a higher Gibbs energy than c-SiNWs, with the energy difference $\triangle G \approx 0.12-0.15$ eV, the a-Si thin film is constantly absorbed at the front In/a-Si interface into the In droplet, while c-SiNW is produced at the rear SiNW/In deposition interface.[25] The growth of SiNWs under different laser powers of 3, 7, 10, and 12 W is shown in Figure 3a–f, with a constant illumination time of 10 min. The results showed that SiNWs started to grow when the power reached up to 7 W, indicating that a related large laser power was needed to build up enough temperature to melt the droplets, against the heat dissipation into the contacted environment. When the power is raised to 10 W, long SiNW arrays can be observed along the guiding edge (Figure 3c,d), with a diameter distribution of 74 ± 9 nm in Figure 3g. More importantly, an obvious gap was found at the end of SiNW and the leading In droplet in this situation (Figure 3f), indicating a typical environmental heating and cooling growth mode.[37] During SiNW growth, the In droplets absorb all of the thin a-Si deposited on their surface and produce SiNWs on the planar surface, with no obvious interface between the a-Si film and the In droplets.

We further measured the temperature elevation on the Si substrate under illumination with different laser powers. As shown in Figure S1 in the Supporting Information, the wafer on glass was placed on the lifting stage to reach a suitable position to be more effectively illuminated and heated by the laser beam shed through the top glass window. Then, a thermocouple was fixed on the wafer to measure the surface temperature, and a black tape was used to shield the thermocouple tip from laser illumination. After that, the laser illumination with different powers was applied on the wafer. The temperature was recorded when it reached a steady-state value. Figure 3k shows that the surface temperature increases with increasing laser power, which can be easily raised to the melting point of In at 156 °C with 3 W irradiation. The

https://doi.org/10.1021/acsanm.4c02962
ACS Appl. Nano Mater. 2024, 7, 16874–16882

Downloaded from pubs.acs.org/aanmf6/article-pdf/7/14/16874/4405546/an4c02962.pdf by NANJING UNIV user on 04 November 2026

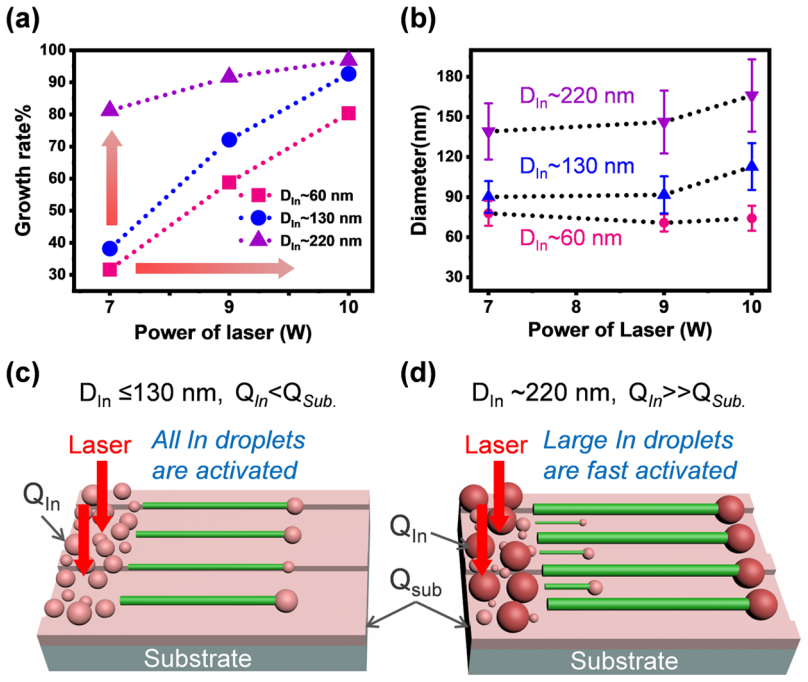


Figure 5. Statistics of growth rate (a) and diameter (b) of SiNWs led by different In droplet sizes. (c, d) The catalyst size-dependent heating mechanism for selective growth and diameter control of SiNWs under laser illumination.

temperature reached a high value of 320 °C when the laser power was set at 10 W, which approximated the temperature used for the growth of IPSLS SiNWs in the substrate heating mode.[34,42] Similarly, we also investigated the guiding growth of SiNWs under 10 W laser illumination, using droplets from 4 and 32 nm thick In, as witnessed in Figures S2 and S3. The apparent gaps were also found at the end of SiNWs and the leading droplets, indicating a substrate heating mode for SiNW growth when using these catalysts. In addition, the geometry of the IPSLS SiNWs is well determined by the ratio of a-Si:H layer thickness to catalyst droplet size.[43] The a-Si layer of ∼20 nm provides a suitable precursor supply for the large In catalyst to guide the growth of straight SiNWs along the edge (Figure S3), while it is too thick for the smaller ones, resulting in the growth of meandering and thin SiNWs (Figure S2).

Interestingly, when the power reached 12 W, all of the In droplets disappeared at the starting and the leading end positions (Figure 3e). This phenomenon can be attributed to the vaporization of the In nanodroplets caused by direct laser heating. Note that the short growth of SiNWs can also be found under this condition, demonstrating that the temperature was gradually increased until it reached the vaporization temperature of In. Briefly, during the high-power laser illumination, the substrate temperature was rapidly increased above the melting point of In of ∼156 °C, and the solid In spheres were transformed into liquid droplets; then the temperature was continuously increased and the In droplets started moving along the guiding edge to produce SiNWs; finally, the temperature reaches up to the vaporization temperature of In due to the constant laser illumination, resulting in the rapid vaporization of the In droplets and growth stop of SiNWs.

In addition, the dynamic growth of SiNWs under a constant laser power of 7 W was examined by SEM, after different growth durations, as shown in Figure 3h−j. The In droplets remained intact during the first 10 s of illumination (Figure 3h), indicating that a necessary incubation time is required for the In droplets to absorb and build up sufficient temperature to melt from the substrate by thermal transmission. Then, the molten droplets started to move and absorb the covered a-Si:H layer to establish a supersaturation of Si atoms in the droplets, triggering the kickoff growth of SiNWs after 30 s of illumination, as seen in Figure 3i. Notably, the very fast activation growth of SiNWs has never been observed in the conventional substrate heating mode, although the heat mode was considered as the substrate heating from laser illumination. After that, all of the In droplets were activated to lead the growth of long SiNWs along the guiding edges, with a length of ∼60 μm, as shown in Figure 3j at t = 5 min. These results demonstrated that the SiNW growth under laser illumination, with an In thickness of 16 nm, was dominated by the substrate heat, while the effect of the direct heat of the In droplets on the growth can be negligible.

Figure 4a−c shows the IPSLS growth of SiNWs under different laser powers of 7, 9, and 12 W, led by the In catalyst droplets formed from an initial thickness of 64 nm. Under the laser power of 7 W, most of the SiNWs seem to stop at more or less the same lengths, as marked by the yellow dashed line in Figure 4a, indicating that the SiNW growth was stopped almost immediately after the laser illumination. According to our previous study,[37] the sudden-growth-stop growth of SiNWs is a typical feature of the self-selected laser-droplet-heating mode, which can be explained by the fact that when the laser was turned off, the In droplets were almost instantly frozen into a solid due to the rapid heat dissipation from the tiny droplets into the large environment. Under a laser power of 9 W, the longer and denser SiNWs were grown along the predefined guiding edges (Figure 4b). From the enlarged image of the growth end (Figure 4d), In droplets were tightly attached to the end of SiNWs, in strong contrast to the droplet-SiNW detaching situation observed in Figure 3f, which is also an important feature of the selected laser-droplet-

Downloaded from pubs.acs.org/aanmf6/article-pdf/7/14/16874/4405546/an4c02962.pdf by NANJING UNIV user on 04 November 2026

https://doi.org/10.1021/acsanm.4c02962
ACS Appl. Nano Mater. 2024, 7, 16874−16882

heating mode. In addition, a typical growth area of ~1 mm^2 and the magnified image of three SiNWs are also shown in the SEM images (Figure S4), demonstrating the potential integration of the IPSLS SiNW channel for Si-based electronics. Furthermore, the moving track of the laser beam can be controlled by a micromotor to achieve line-by-line laser-induced droplet heating, enabling the scalable growth of SiNW arrays on large-area substrates. When the laser power reached up to 10 W, all of the guiding edges were filled with thick SiNWs, with a length of ~185 nm (Figure 4c) and a diameter of 166 ± 27 nm (Figure 4f). These results indicated that the larger catalyst droplets can indeed easily absorb the NIR laser and facilitate the fast guiding growth of SiNWs, while the temperature elevation of the substrate produced by laser illumination had little effect on the growth of large SiNWs. This unique capability can also be demonstrated by a simple experiment. The catalyst pads with nominal thicknesses of 32 and 64 nm were deposited on polyimide (PI) substrate, and then the NIR laser with a power of 10 W was illuminated on the films. Figure 4e indicates that the laser leads to serious deterioration and dissociation of the underlying PI thin film with the 64 nm thick catalyst, resulting in reduced transparency and cascading burning spreading from the region below the In pads. In comparison, the PI substrate remains intact when the 10 W laser illumination was applied to the catalyst pad with 32 nm thickness (Figure S3d). Note that the high temperature in growth zones can be effectively separated from the underlying PI thin film by the use of a SiO_2 buffer layer before they can be used to fabricate the electronics.[37] Thanks to the high evaporation point of the large droplets, the temperature on these In droplets did not lead to their disappearance during the growth of SiNWs.

To examine the crystallinity of SiNWs grown by laser heating, a cross section of the nanowire was prepared by focused ion beam (FIB) milling (as shown in Figure 4g) and then characterized by high-resolution transmission electron microscopy (HR-TEM). Close HR-TEM examination (Figure 4h) showed that the as-grown SiNW had a crystalline lattice with a clear fringe spacing of 0.31 nm, corresponding to that of the Si (111) planes. According to the electron diffraction pattern shown in Figure 4i, a set of coherent Si lattices was observed, with a growth orientation along the Si [110] direction, which was consistent with the TEM results in our previous report.[37]

Furthermore, the growth rate and diameter of SiNWs heated by an NIR laser, led by different In droplet sizes, are shown in Figure 5a,b. The growth rates highly depend on the laser intensity and the catalyst sizes. Specifically, the growth rate of SiNWs guided by large droplet size of ~220 nm was almost two times higher than those of ~130 and ~60 nm with the same laser power of 7 W, which can be attributed to the high temperature directly generated by the large droplets under laser illumination. However, the temperature was insufficient to activate the In droplets with a diameter of <130 nm for SiNW growth, due to the low substrate heating effect in this situation. Fortunately, the growth rate can be significantly improved by increasing the laser intensity. For example, the growth rate under 10 W illumination was two times higher than that at 7 W. Similarly, the diameter of the as-grown SiNWs also depended on the laser intensity and the catalyst size. In addition, the SiNW diameter produced by the droplet size of <130 nm was smaller than that by the large droplets of ~220 nm, which can be attributed to the fact that the diameter of as-grown SiNWs is roughly proportional to the size of leading droplets.

Similar to the photothermal conversion in popular metal nanomaterials, such as gold and silver particles, the selected heating of In nanodroplets under laser illumination can also be explained by surface plasmon resonance. When the incident light irradiates conductive In droplets, the light interacts with free electrons or holes in In and causes a coherent oscillation. The electrons jump to an excited energy state, followed by the electron−electron scattering, thereby leading to the redistribution of hot electrons.[44,45] Hot electrons can release thermal energy through the process of electron−phonon relaxation, which produces photothermal heating of the In nanodroplets.

Theoretically, the heat (Q_{In}, W) generated on spherical In nanodroplets under laser illumination can be described as $Q_{In} = C_{abs} \cdot I$,[46] where C_{abs} is the absorption cross-section area and can be quantitatively derived as $C_{abs} \propto V_{In.} \propto R_{In.}^3$,[47] and I is the laser fluence. Considering the heat transfer with the surrounding medium, the temperature elevation (ΔT_{In}) of the spherical In droplets can be calculated by $\Delta T_{In} = Q_{In}/4\pi K_s R_{In}$,[48,49] where K_s is the thermal conductivity of the surrounding medium. Therefore, the temperature elevation on In nanodroplets heated directly by the laser is proportional to the catalyst size R_{In} (or D_{In}). This unique capability results in different growth modes of IPSLS SiNWs. Specifically, Figure 5c shows the schematic of SiNW growth via substrate heating mode when the leading In droplets are small (e.g., ≤130 nm), where Q_{In} is very small and insufficient to directly melt the droplets. During this course, the fast heating of silicon substrate under continuous laser illumination transfers the heat to the above droplets and melts all of the small catalysts to guide the growth of thin SiNWs (also shown in Figure 3g). In contrast, the selective and direct heating of the large-size droplets with 220 nm makes them fast moving and leads to the growth of large SiNWs (Figure 5d). Note that substrate heating also plays an important role in the heating of small droplets among the large ones, resulting in a guiding growth of small and relatively short SiNWs, which can be witnessed by the image of SiNW at the stating position in Figure S5. Considering the integration of SiNW channels for high-performance FETs, the high-quality and thin-diameter SiNWs, grown by selected laser-droplet-heating mode, are required, which can be achieved by modulating the wavelength and power of the laser and the size of the leading droplets.

CONCLUSIONS

In summary, the effect of catalyst size-dependent heating on the controlled growth of IPSLS SiNWs under laser illumination has been established. The growth rate and diameter of as-grown SiNWs under laser illumination were determined by the droplet size and laser powers. For the leading growth of SiNWs by small size of droplets, the substrate heating dominates the SiNW growth with a diameter of 74 ± 9 nm, while the direct laser heating effect on droplets can be neglected. We also found that the large catalyst droplets were directly heated to a high temperature by laser to guide the SiNW growth with a large diameter of 166 ± 27 nm, while the small droplets among the large droplets were still heated through substrate heating mode and led the growth of small SiNWs. Thus, this study develops a new approach for diameter control of IPSLS SiNWs and provides a solid material basis for the construction of Si-based electronics.

Downloaded from pubs.acs.org/aanmf6/article-pdf/7/14/16874/4405546/an4c02962.pdf by NANJING UNIV user on 04 November 2026

https://doi.org/10.1021/acsanm.4c02962
ACS Appl. Nano Mater. 2024, 7, 16874−16882

EXPERIMENTAL SECTION

Catalyst Deposition and the Droplet Formation. A silicon wafer coated with 500 nm thick SiO_2 was first cleaned sequentially with acetone, ethanol, and deionized water for 10 min each in an ultrasonic cleaning machine. Then, the straight guiding step edges were defined on the substrate surface by photolithography and etched into the SiO_2 layer to a depth of ∼150 nm using inductively coupled plasma. After that, the region for the In catalyst was patterned by lithography at the end of the guiding edge. The In films with different thicknesses were deposited by thermal evaporation and followed by a lift-off procedure in acetone solution. Then, the samples were loaded into the PECVD system and treated with H-plasma at 250 °C for 5 min to remove the native surface In oxide layer and to melt and agglomerate them into discrete droplets at a pressure of 140 Pa and a radio frequency power of 10 W.

Laser Illumination for the IPSLS Growth of SiNWs. An amorphous silicon (a-Si) layer with a thickness of ∼20 nm was deposited at 150 °C (below the melting point of In) using SiH_4 plasma for 4 min at a flow rate of SiH_4 and a pressure of 5 SCCM and 20 Pa, respectively. Then, laser illumination was applied to the samples in a vacuum, with different powers and durations. Briefly, the selected lasers with powers of 3, 7, 10, and 12 W were separately irradiated on the different samples for 10 min each. For the dynamic growth of SiNWs under laser heating, the 7 W laser was applied to the samples with an illumination time of 10 s, 30 s, or 5 min. The In droplets molten again and started to move along the guiding edges, absorbing the nearby a-Si layer to produce crystalline SiNWs. The morphologies of the as-grown SiNWs were collected in SEM. The crystalline lattice and growth direction of SiNWs were characterized by TEM, where a focused ion beam (FIB) milling was first used to cut a cross-sectional slice of SiNW. The growth rate and diameter of SiNWs under different laser powers were obtained from the statistical results in SEM images.

Finite Element Simulation of Size-Dependent Catalyst Heating under Laser Illumination. The heating capacity of In droplets with different diameters was determined using COMSOL simulation toolkits. The In droplets with diameters of D_{In} = 100 and 300 nm were constructed on Si wafers, with the a-Si film and the c-SiNW at the front and back interface, respectively. The power of the 808 nm laser was assumed to be 10 W.

ASSOCIATED CONTENT

Supporting Information

The Supporting Information is available free of charge at https://pubs.acs.org/doi/10.1021/acsanm.4c02962.

The temperature raising testing on SiO_2-coated Si wafer with laser illumination; SEM images of the as-grown SiNWs led by In droplets from In thickness of 4 nm, with the laser power of 10 W for 10 min; The SEM image of the as-grown SiNWs led by In droplets with D_{In} of 130 nm from In thickness of 32 nm, with the laser powers of 7 and 10 W for 10 min. The optical images of catalyst film-coated PI substrate after laser illumination with the power of 10 W for 10 min; Typical growth of SiNW arrays with an area of ∼1 mm^2 under 10 W illumination; The SEM image of SiNWs at the starting position, led by the large catalysts from T_{In} of 64 nm (PDF)

AUTHOR INFORMATION

Corresponding Authors

Zongguang Liu − *College of Physics Science and Technology/ Microelectronics Industry Research Institute, Yangzhou University, 225009 Yangzhou, China;* orcid.org/0000-0003-4141-7462; Email: zgliu@yzu.edu.cn

Linwei Yu − *School of Electronic Science and Engineering/ National Laboratory of Solid-State Microstructures, Nanjing University, 210023 Nanjing, China;* orcid.org/0000-0002-0801-5210; Email: yulinwei@nju.edu.cn

Authors

Yinzi Cheng − *School of Electronic Science and Engineering/ National Laboratory of Solid-State Microstructures, Nanjing University, 210023 Nanjing, China*

Ruijin Hu − *College of Physics Science and Technology/ Microelectronics Industry Research Institute, Yangzhou University, 225009 Yangzhou, China;* orcid.org/0009-0006-5973-6954

Junzhuan Wang − *School of Electronic Science and Engineering/National Laboratory of Solid-State Microstructures, Nanjing University, 210023 Nanjing, China*

Jun Xu − *School of Electronic Science and Engineering/ National Laboratory of Solid-State Microstructures, Nanjing University, 210023 Nanjing, China;* orcid.org/0000-0002-0469-9766

Complete contact information is available at: https://pubs.acs.org/10.1021/acsanm.4c02962

Notes

The authors declare no competing financial interest.

ACKNOWLEDGMENTS

The authors acknowledge the financial support received from the National Natural Science Foundation of China under grant no. 62104100, the National Key Research Program of China under no. 92164201, and the National Natural Science Foundation of China for Distinguished Young Scholars under no. 62325403.

REFERENCES

(1) Wang, D.; Sheriff, B. A.; Heath, J. R. Complementary Symmetry Silicon Nanowire Logic: Power-Efficient Inverters with Gain. *Small* **2006**, *2* (10), 1153−1158.

(2) Huang, R.-G.; Tham, D.; Wang, D.; Heath, J. R. High performance ring oscillators from 10-nm wide silicon nanowire field-effect transistors. *Nano Res.* **2011**, *4*, 1005−1012.

(3) Li, X.; Yu, B.; Wang, B.; Bi, R.; Li, H.; Tu, K.; Chen, G.; Li, Z.; Huang, R.; Li, M. Complementary Photo-Synapses Based on Light-Stimulated Porphyrin-Coated Silicon Nanowires Field-Effect Transistors (LPSNFET). *Small* **2021**, *17* (30), No. 2101434.

(4) Weber, W. M.; Mikolajick, T. Silicon and germanium nanowire electronics: physics of conventional and unconventional transistors. *Rep. Prog. Phys.* **2017**, *80* (6), No. 066502.

(5) Cui, Y.; Zhong, Z.; Wang, D.; Wang, W. U.; Lieber, C. M. High performance silicon nanowire field effect transistors. *Nano Lett.* **2003**, *3* (2), 149−152.

(6) Schütt, J.; Ibarlucea, B.; Illing, R.; Zörgiebel, F.; Pregl, S.; Nozaki, D.; Weber, W. M.; Mikolajick, T.; Baraban, L.; Cuniberti, G. Compact nanowire sensors probe microdroplets. *Nano Lett.* **2016**, *16* (8), 4991−5000.

(7) Adam, T.; Hashim, U. Highly sensitive silicon nanowire biosensor with novel liquid gate control for detection of specific single-stranded DNA molecules. *Biosens. Bioelectron.* **2015**, *67*, 656−661.

(8) Shehada, N.; Cancilla, J. C.; Torrecilla, J. S.; Pariente, E. S.; Brönstrup, G.; Christiansen, S.; Johnson, D. W.; Leja, M.; Davies, M. P.; Liran, O.; et al. Silicon nanowire sensors enable diagnosis of patients via exhaled breath. *ACS Nano* **2016**, *10* (7), 7047−7057.

Downloaded from pubs.acs.org/aanmf6/article-pdf/7/14/16874/4405546/an4c02962.pdf by NANJING UNIV user on 04 November 2026

(9) Zhao, Y.; You, S. S.; Zhang, A.; Lee, J.-H.; Huang, J.; Lieber, C. M. Scalable ultrasmall three-dimensional nanowire transistor probes for intracellular recording. *Nat. Nanotechnol.* **2019**, *14* (8), 783−790.
(10) Chen, K.-I.; Li, B.-R.; Chen, Y.-T. Silicon nanowire field-effect transistor-based biosensors for biomedical diagnosis and cellular recording investigation. *Nano Today* **2011**, *6* (2), 131−154.
(11) Park, I.; Li, Z.; Li, X.; Pisano, A. P.; Williams, R. S. Towards the silicon nanowire-based sensor for intracellular biochemical detection. *Biosens. Bioelectron.* **2007**, *22* (9−10), 2065−2070.
(12) Koo, S.-M.; Li, Q.; Edelstein, M. D.; Richter, C. A.; Vogel, E. M. Enhanced channel modulation in dual-gated silicon nanowire transistors. *Nano Lett.* **2005**, *5* (12), 2519−2523.
(13) Gao, Z.; Agarwal, A.; Trigg, A. D.; Singh, N.; Fang, C.; Tung, C.-H.; Fan, Y.; Buddharaju, K. D.; Kong, J. Silicon nanowire arrays for label-free detection of DNA. *Analytical chemistry* **2007**, *79* (9), 3291−3297.
(14) Yu, X.; Wang, Y.; Zhou, H.; Liu, Y.; Wang, Y.; Li, T.; Wang, Y. Top-down fabricated silicon-nanowire-based field-effect transistor device on a (111) silicon wafer. *Small* **2013**, *9* (4), 525−530.
(15) Mojarad, N.; Gobrecht, J.; Ekinci, Y. Interference lithography at EUV and soft X-ray wavelengths: Principles, methods, and applications. *Microelectron. Eng.* **2015**, *143*, 55−63.
(16) Rosa, A. M.; Leonhardt, A.; de Souza, L. O.; Lima, L. P. B.; dos Santos, M. V. P.; Manera, L. T.; Diniz, J. A. A novel self-aligned double patterning integrated with Ga+ focused ion beam milling for silicon nanowire definition. *Microelectron. Eng.* **2021**, *237*, No. 111493.
(17) Akbari-Saatlu, M.; Procek, M.; Mattsson, C.; Thungström, G.; Nilsson, H.-E.; Xiong, W.; Xu, B.; Li, Y.; Radamson, H. H. Silicon nanowires for gas sensing: A review. *Nanomaterials* **2020**, *10* (11), 2215.
(18) Nguyen, T.; Hsu, C. H.; Lien, D. H.; Su, Y. S. Economical Silicon Nanowire Growth via Cooling Controlled Solid−Liquid−Solid Mechanism. *Adv. Mater. Interfaces* **2023**, *10* (6), No. 2202247.
(19) Cheng, J.; Jiang, S.; Fan, J.; Yao, J.; Du, N.; Li, X.; Wang, D.; Dong, P.; Zhou, Z.; Zhang, Y. Research on synthesis and nucleation mechanism of silicon nanowire by silver catalysis in molten salt. *Ceram. Int.* **2023**, *49* (11), 18776−18785.
(20) Wagner, R. S.; Ellis, W. Vapor-liquid-solid mechanism of single crystal growth. *Appl. Phys. Lett.* **1964**, *4* (5), 89−90.
(21) Cui, Y.; Lauhon, L. J.; Gudiksen, M. S.; Wang, J.; Lieber, C. M. Diameter-controlled synthesis of single-crystal silicon nanowires. *Appl. Phys. Lett.* **2001**, *78* (15), 2214−2216.
(22) Wu, Y.; Cui, Y.; Huynh, L.; Barrelet, C. J.; Bell, D. C.; Lieber, C. M. Controlled growth and structures of molecular-scale silicon nanowires. *Nano Lett.* **2004**, *4* (3), 433−436.
(23) Shan, Y.; Kalkan, A. K.; Peng, C.-Y.; Fonash, S. J. From Si source gas directly to positioned, electrically contacted Si nanowires: the self-assembling "grow-in-place" approach. *Nano Lett.* **2004**, *4* (11), 2085−2089.
(24) Shan, Y.; Fonash, S. J. Self-assembling silicon nanowires for device applications using the nanochannel-guided "grow-in-place" approach. *ACS Nano* **2008**, *2* (3), 429−434.
(25) Sun, Y.; Dong, T.; Yu, L.; Xu, J.; Chen, K. Planar growth, integration, and applications of semiconducting nanowires. *Adv. Mater.* **2020**, *32* (27), No. 1903945.
(26) Yu, L.; Alet, P.-J.; Picardi, G.; Roca i Cabarrocas, P. An In-plane solid-liquid-solid growth mode for self-avoiding lateral silicon nanowires. *Phys. Rev. Lett.* **2009**, *102* (12), No. 125501.
(27) Yu, L.; Roca i Cabarrocas, P. Initial nucleation and growth of in-plane solid-liquid-solid silicon nanowires catalyzed by indium. *Phys. Rev. B* **2009**, *80* (8), No. 085313.
(28) Yu, L.; Chen, W.; O'Donnell, B.; Patriarche, G.; Bouchoule, S.; Pareige, P.; Rogel, R.; Claire Salaun, A.; Pichon, L.; Roca i Cabarrocas, P. Growth-in-place deployment of in-plane silicon nanowires. *Appl. Phys. Lett.* **2011**, *99* (20), No. 203104.
(29) Song, X.; Zhang, T.; Wu, L.; Hu, R.; Qian, W.; Liu, Z.; Wang, J.; Shi, Y.; Xu, J.; Chen, K.; Yu, L. Highly Stretchable High-Performance Silicon Nanowire Field Effect Transistors Integrated on Elastomer Substrates. *Adv. Sci.* **2022**, *9* (9), No. 2105623.
(30) Xu, M.; Wang, J.; Xue, Z.; Wang, J.; Feng, P.; Yu, L.; Xu, J.; Shi, Y.; Chen, K.; Roca i Cabarrocas, P. High performance transparent in-plane silicon nanowire Fin-TFTs via a robust nano-droplet-scanning crystallization dynamics. *Nanoscale* **2017**, *9* (29), 10350−10357.
(31) Hu, R.; Liang, Y.; Qian, W.; Gan, X.; Liang, L.; Wang, J.; Liu, Z.; Shi, Y.; Xu, J.; Chen, K.; Yu, L. Ultra-Confined Catalytic Growth Integration of Sub-10 nm 3D Stacked Silicon Nanowires Via a Self-Delimited Droplet Formation Strategy. *Small* **2022**, *18* (42), No. 2204390.
(32) Yin, H.; Yang, H.; Xu, S.; Pan, D.; Xu, J.; Chen, K.; Yu, L. High performance Si nanowire TFTs with ultrahigh on/off current ratio and steep subthreshold swing. *IEEE Electron Device Lett.* **2020**, *41* (1), 46−49.
(33) Song, X.; Hu, R.; Xu, S.; Liu, Z.; Wang, J.; Shi, Y.; Xu, J.; Chen, K.; Yu, L. Highly sensitive ammonia gas detection at room temperature by integratable silicon nanowire field-effect sensors. *ACS Appl. Mater. Interfaces* **2021**, *13* (12), 14377−14384.
(34) Liu, Z.; Yan, J.; Ma, H.; Hu, T.; Wang, J.; Shi, Y.; Xu, J.; Chen, K.; Yu, L. Ab initio design, shaping, and assembly of free-standing silicon nanoprobes. *Nano Lett.* **2021**, *21* (7), 2773−2779.
(35) Yan, J.; Zhang, Y.; Liu, Z.; Wang, J.; Xu, J.; Yu, L. Ultracompact single-nanowire-morphed grippers driven by vectorial Lorentz forces for dexterous robotic manipulations. *Nat. Commun.* **2023**, *14* (1), No. 3786.
(36) Zhang, Y.; Yan, J.; Li, D.; Qian, W.; Qi, Y.; Wu, L.; Liu, Z.; Wang, J.; Xu, J.; Yu, L. Single-nanowire-morphed mechanical slingshot for directional shooting delivery of micro-payloads. *Nanotechnology* **2023**, *34* (41), No. 415604.
(37) Zhang, T.; Hu, R.; Zhang, S.; Liu, Z.; Wang, J.; Xu, J.; Chen, K.; Yu, L. Superfast growth dynamics of high-quality silicon nanowires on polymer films via self-selected laser-droplet-heating. *Nano Lett.* **2021**, *21* (1), 569−576.
(38) Hu, R.; Xu, S.; Wang, J.; Shi, Y.; Xu, J.; Chen, K.; Yu, L. Unprecedented uniform 3d growth integration of 10-layer stacked si nanowires on tightly confined sidewall grooves. *Nano Lett.* **2020**, *20* (10), 7489−7497.
(39) Cheng, Y.; Gan, X.; Liu, Z.; Wang, J.; Xu, J.; Chen, K.; Yu, L. Nanostripe-Confined Catalyst Formation for Uniform Growth of Ultrathin Silicon nanowires. *Nanomaterials* **2023**, *13* (1), 121.
(40) Cheng, Y.; Liu, Z.; Wang, J.; Xu, J.; Yu, L. Deterministic Single-Row-Droplet Catalyst Formation for Uniform Growth Integration of High-Density Silicon Nanowires. *ACS Appl. Mater. Interfaces* **2024**, *16* (18), 23625−23633.
(41) Yuan, R.; Qian, W.; Liu, Z.; Wang, J.; Xu, J.; Chen, K.; Yu, L. Designable integration of silicide nanowire springs as ultra-compact and stretchable electronic interconnections. *Small* **2021**, *18* (6), No. 2104690.
(42) Yuan, R.; Qian, W.; Liu, Z.; Wang, J.; Xu, J.; Chen, K.; Yu, L. Designable Integration of Silicide Nanowire Springs as Ultra-Compact and Stretchable Electronic Interconnections. *Small* **2022**, *18* (6), No. 2104690.
(43) Sun, Y.; Dong, T.; Wang, J.; Xu, J.; Chen, K.; Roca i Cabarrocas, P.; Yu, L. Meandering growth of in-plane silicon nanowire springs. *Appl. Phys. Lett.* **2019**, *114* (23), No. 233103.
(44) Chen, J.; Ye, Z.; Yang, F.; Yin, Y. Plasmonic nanostructures for photothermal conversion. *Small Science* **2021**, *1* (2), No. 2000055.
(45) Yan, T.; Su, M.; Wang, Z.; Zhang, J. Second Near-Infrared Plasmonic Nanomaterials for Photoacoustic Imaging and Photothermal Therapy. *Small* **2023**, *19* (30), No. 2300539.
(46) Qin, Z.; Bischof, J. C. Thermophysical and biological responses of gold nanoparticle laser heating. *Chem. Soc. Rev.* **2012**, *41* (3), 1191−1217.
(47) Kim, M.; Lee, J. H.; Nam, J. M. Plasmonic photothermal nanoparticles for biomedical applications. *Adv. Sci.* **2019**, *6* (17), No. 1900471.

Downloaded from pubs.acs.org/aanmf6/article-pdf/7/14/16874/4405546/an4c02962.pdf by NANJING UNIV user on 04 November 2026

(48) Baffou, G.; Quidant, R.; García de Abajo, F. J. Nanoscale control of optical heating in complex plasmonic systems. *ACS Nano* **2010**, *4* (2), 709−716.
(49) Baffou, G.; Quidant, R. Thermo-plasmonics: using metallic nanostructures as nano-sources of heat. *Laser Photonics Rev.* **2013**, *7* (2), 171−187.

Downloaded from pubs.acs.org/aanmf6/article-pdf/7/14/16874/4405546/an4c02962.pdf by NANJING UNIV user on 04 November 2026

https://doi.org/10.1021/acsanm.4c02962
ACS Appl. Nano Mater. 2024, 7, 16874−16882